https://doi.org/10.15302/J-LAF-0-020031 Received Date | 2023-12-27 Accepted Date | 2024-06-07

Examining the Heterogeneity of Geographical and Social Equity of Urban Green Space Exposure at Overhead and Eye Levels

Yingyi CHENG[1], Zhaowu YU[2,*], Jinguang ZHANG[1]

1 College of Landscape Architecture, Nanjing Forestry University, Nanjing 210037, China
2 Department of Environmental Science and Engineering, Fudan University, Shanghai 200438, China

*CORRESPONDING AUTHOR
Address: No. 220 Handan Road, Yangpu District, Shanghai 200438, China
Email: zhaowu_yu@fudan.edu.cn

GRAPHICAL ABSTRACT

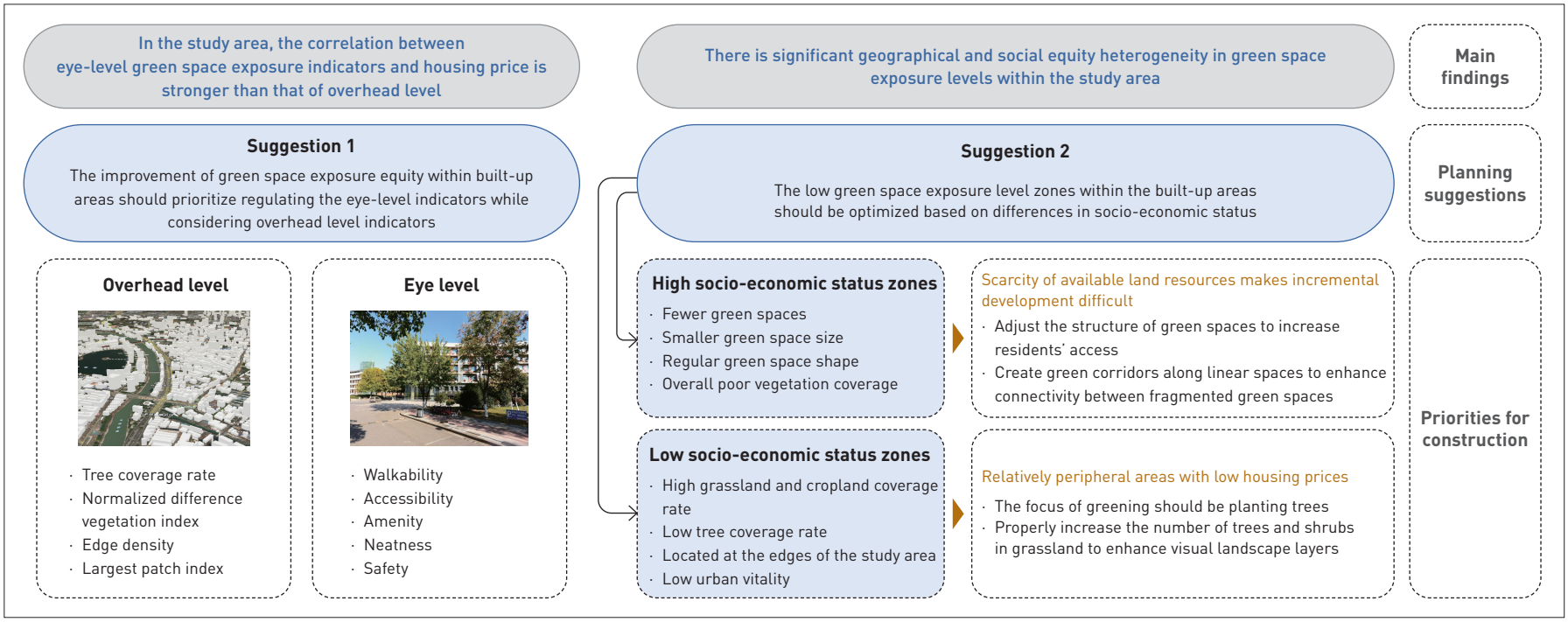

ABSTRACT

Enhancing green space exposure is a crucial strategy for proactively intervening in public health from an upstream perspective. However, the distribution of green spaces in urban areas is often uneven, leading to issues such as "green inequity." This study aims to systematically assess the level of green space exposure at overhead and eye levels, analyze the geographical and social equity of green space exposure, and propose planning and regulatory strategies. Focusing on Nanjing as the study area, the research team first constructed a green space exposure assessment system based on the composition and configuration of urban green spaces at the overhead level, and the quantity and perceived quality of street green space at the eye level, assessing the geographical equity of green space exposure. Next, by selecting housing price as a socio-economic indicator, the research used various spatial regression models to analyze the spatial correlation between green space exposure and housing price, evaluating the social equity of green space exposure. The research finds 1) significant imbalances in both the geographical and social equity of green space exposure within the study area; 2) the spatial correlation between eye-level green space exposure indicators and housing price ranges from 0.08 to 0.29, generally higher than that at overhead level (ranging from 0.02 to 0.13); 3) significant heterogeneity in the spatial correlation between green space exposure and housing price, with people in higher-priced housing being more likely to benefit from green space services. The results can accurately identify blind spots in green space exposure and imbalance areas between green space supply and socio-economic status, providing guidance for "scientific greening," and further promoting empirical studies in Exposure Ecology.

KEYWORDS

Exposure Ecology; Green Space Exposure; Urban Green Spaces; Geographical Equity; Social Equity; Spatial Regression Model

HIGHLIGHTS

- Develops an urban green space exposure assessment framework, including indicators at both overhead and eye levels
- Evaluates the social equity of urban green space exposure using four spatial regression models
- Identifies spatial correlations between housing price and green space exposure indicators at overhead and eye levels
- Proposes improvements for areas with varying green space exposure levels based on spatial regression results

RESEARCH FUNDS

- Project of "A Multi-Scale Coupling Study on the Threshold Efficiency of Urban Green Spaces in Mitigating Urban Heat," National Natural Science Foundation of China (No. 42171093)
- Project of "A Study on the Spatial Allocation Levels and Mechanisms of Public Service Facilities in Urban Residential Areas Integrating Diverse Needs," Young Scientists Fund of the National Natural Science Foundation of China (No. 42201200)
- Project of "A Study on the Threshold Measurement and Influencing Factors of Physiological Health Effects of Urban Population Exposure to Green Spaces," Young Scientists Fund of the National Natural Science Foundation of China (No. 42401103)
- Project of "A Study on the Mitigation Effects of Urban Green Vegetation on Thermal Environments at Multiple Scales," Natural Science Foundation of Shanghai (No. 21ZR1408500)
- Project of "A Study on the Cooling Efficiency Threshold and Energy Dynamics Mechanism of Urban Green Spaces Under Typical Climatic Conditions," Shanghai Pujiang Program (No. 21PJ1401600)
- Project of "A Systematic Measurement and Optimal Allocation of Green Space Exposure Levels for Healthy Cities," Natural Science Foundation of the Jiangsu Higher Education Institutions of China (No. 22KJB220006)

EDITED BY Yuting GAO, Xidong MA
TRANSLATED BY Yuting GAO

1 Introduction

Green spaces, as critical urban ecological features, are essential for constructing resilient cities and improving the quality of life[1][2]. These spaces not only provide extensive ecosystem services but also offer vital venues for residents to connect with and experience nature[3][4]. However, in urban contexts, particularly in high-density areas, green spaces are scarce and often unevenly distributed, leading to a series of equity-related challenges[5][6].

Green space exposure (GSE) refers to direct or indirect access and interaction between residents and urban green spaces[7]. Ensuring sufficient exposure to urban green spaces is a prerequisite for promoting health benefits[8]. Over the years, both domestic and international scholars have explored the characteristics of urban GSE, including its spatial patterns and health effect measurements[9][10]. Current GSE assessments are predominantly conducted at the overhead level, utilizing indicators such as area of green space, normalized difference vegetation index, percentage of tree canopy, and percentage of vegetation[11]~[13]. Some studies also evaluate the configuration of green spaces, e.g., fragmentation, shape complexity, and patch cohesion[14][15]. However, such studies primarily rely on satellite imagery to reveal large-scale spatiotemporal GSE patterns, omitting the vertical dimension of exposure or the actual spatiotemporal behaviors of residents in urban green spaces. Consequently, these studies fail to reflect the inherent complexity, diversity, and dynamism of GSE. With the advancement of big data and machine learning technologies, scholars have begun to preliminarily explore eye-level GSE metrics, such as using street view images to measure the green view index and quantify the quality of street spaces[16][17]. Although there has been a shift from single-dimensional measurements to multi-dimensional GSE evaluations[9][18][19], comprehensive urban GSE assessment models remain scarce. Bin Chen et al. have emphasized the importance of integrating green space quantity, quality, type, and structure attributes in quantitative studies and advocated for GSE measurements that consider spatial, temporal, and social disparities[20]. Theoretically, Zhaowu Yu et al. proposed the framework of Exposure Ecology to systematically understand the nexus of (urban) natural ecosystems, ecological exposure, and health[21]. Geographical and social equity in urban GSE is a critical study component of this framework, focusing on the "object–reality" dimension.

Green space equity research has evolved from quantity equity to spatial distribution equity, and to social equity[22]. Early studies predominantly employed conventional green space coverage

indicators (e.g., ratio of green space, per capita green area) to assess the service capacity of green spaces in a given administrative area. While these metrics reveal the supply levels, they often fail to reflect the demand–supply relationship between populations and green spaces[20][23]. Later studies incorporating population distribution and socio-economic attributes into GSE equity analyses have gained prominence[24][25]. Evidence suggests that GSE equity varies across different geographic regions and socio-cultural contexts[26]. Inequities in GSE potentially exacerbate health disparities, particularly among socio-economically disadvantaged groups[27]. The United Nations' Sustainable Development Goals proposes to "provide universal access to safe, inclusive and accessible, green and public spaces, in particular for women and children, older persons and persons with disabilities"[28]. Systematically assessing urban GSE, identifying blind spots, understanding geographical and social disparities, and proposing planning interventions are pivotal for achieving green space growth scientifically and for upstream public health interventions[29]. Despite growing interest, existing research lacks comprehensive evaluations of both geographical and social equity of GSE in high-density urban areas, limiting the ability to propose targeted optimization strategies for diverse urban contexts.

Building on the framework of Exposure Ecology, this study aims to construct an assessment system for urban GSE at both overhead and eye levels. It seeks to systematically evaluate the geographical and social equity of urban GSE and address the following questions: 1) What are the spatial distribution characteristics of urban GSE indicators at overhead and eye levels? 2) Is there any spatial correlation and heterogeneity between GSE indicators and housing price?

2 Research Methods

2.1 Study Area

This study focuses on the central urban area of Nanjing City, China (Fig. 1). By the end of 2022, Nanjing had a total population of approximately 9.5 million, with 8.26 million urban population[30]. According to the Master plan of Nanjing Territorial Spatial Planning (2021–2035), the central urban area encompasses four centers: Xinjiekou, Hexi, Chengnan, and Jiangbei, covering a total planned area of 804 km^2. The study area has a prosperous economy and plays a critical role in culture and history as it covers the cultural core of ancient capital. It also features the highest population density and the most intricate road network in the city. This research divided the study area into 500 m × 500 m fishnet grids using ArcGIS 10.3, with each grid as a sample unit.

2.2 Construction of the Urban GSE Assessment Model

This research developed an urban GSE assessment system at both overhead and eye levels. The overhead-level indicators include two categories: green space composition and configuration (Table 1). The eye-level indicators consist of two categories: quantity and perceived quality (Table 2).

2.2.1 Selection and Data Acquisition of Overhead-Level GSE Indicators

This research first downloaded Sentinel-2 satellite imagery (10 m resolution) of September 2021 via the Copernicus Open Access Hub. The NDVI for the study area was calculated using the Sentinel Application Platform (SNAP) and ArcGIS 10.3. Next, the data of green space composition indicators were derived from the European Space Agency's WorldCover v100 land cover dataset (10 m resolution) and calculated with Fragstats 4.2, identifying eight land cover types: tree, shrub, grassland, cropland, built-up land, bare/sparsely vegetated land, water body, and herbaceous wetland. Given the minimal area proportions of shrubland (0.001%) and herbaceous wetland (0.013%), only the coverage rates of tree, grassland, and cropland were included in the GSE composition indicators. The landscape pattern indices of tree, grassland, and cropland as a whole were calculated using Fragstats 4.2 as configuration dimension indicators.

1. Location of the study area.

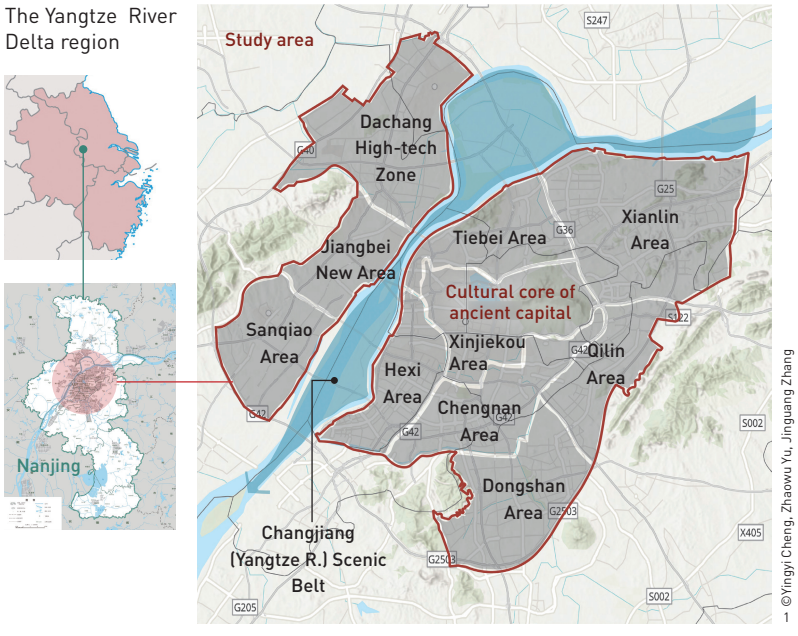

©Yingyi Cheng, Zhaowu Yu, Jinguang Zhang
1

Table 1: Overhead-level GSE indicators

Category	Indicator	Description
Composition	Normalized difference vegetation index (NDVI)	· A reflection of vegetation density and health of the ground vegetation · Higher values indicate higher vegetation density and healthier condition
	Tree coverage rate	Proportion of tree area in the grid
	Grassland coverage rate	Proportion of grassland area in the grid
	Cropland coverage rate	Proportion of cropland area in the grid
	Percentage of landscape (PLAND)	The ratio of the total area of green space patches to the total area in the grid
Configuration	Largest patch index (LPI)	· The ratio of the area of the largest green space patch to the area of the grid · Values closer to 0 indicate smaller patches
	Number of patches (NP)	· Number of green space patches in the grid · Higher values indicate greater fragmentation
	Edge density (ED)	· The ratio of the total edge length of all green space patches to the area of the grid · Higher values indicate greater fragmentation
	Shape index (SHAPE)	· Average shape index (ratio of the patch perimeter to the circumference of a circle with the same area) of all green space patches in the grid · Values closer to 0 indicate simpler shapes
	Fractal dimension index (FRAC)	· Average edge complexity of all green space patches in the grid · Values closer to 0 indicate simpler shapes
	Patch cohesion index (COHESION)	· Degree of aggregation of green space patches · Values closer to 0 indicate simpler shapes

Table 2: Eye-level GSE indicators

Category	Indicator	Description
Quantity	Green view index (*GVI*)	Percentage of vegetation in a person's field of view
Perceived quality	Vegetation abundance	Diversity of plant species in street green spaces
	Walkability	Degree to which the street environment supports walking activities
	Accessibility	Ease with which people can reach and use street green spaces
	Amenity	Convenience of facilities and services provided in street green spaces
	Openness	Connectivity and openness of the street network
	Neatness	Cleanliness of green spaces
	Safety	Safety conditions of street green spaces, including objective factors (e.g., crime rate, nighttime lighting, and emergency facilities) and subjective perceptions of the street atmosphere

2.2.2 Selection and Data Acquisition of Eye-level GSE Indicators

First, this research employed ArcGIS to establish 79,777 observation points at 200-meter intervals along the first class, second class, and third class roads. Street view images from Baidu Maps were adopted to capture images in four cardinal directions (0°, 90°, 180°, and 270°) at each observation point, resulting in a total of 319,108 images (640 × 480 pixels). Next, a fully convolutional network model (FCN-8s) was trained in Python 3.7 based on the ADE20K dataset, which includes 150 object categories (e.g., trees, buildings, cars). The images were semantically segmented to identify their compositional elements. Pixels corresponding to different semantics were filled with specific colors, and the percentage of pixels representing vegetation was calculated to determine the *GVI*:

$$GVI = \frac{\sum_{i=1}^{m} Area_g}{\sum_{i=1}^{m} Area_t} \times 100\%, \quad (1)$$

where $Area_t$ represents the total number of pixels in each street view image, $Area_g$ is the number of pixels occupied by vegetation, and m is the number of images captured at each observation point (4 in this research).

To evaluate people's perceived quality of the street view images, a human-machine adversarial scoring method was employed. The research team randomly selected 5,000 street-view images from

the database, covering various landscape features, to construct a training dataset (Fig. 2). Forty volunteers (1:1 male-to-female ratio) were randomly recruited from university researchers specializing in landscape architecture, architecture, and urban planning, as well as from local shopkeepers familiar with the area. Volunteers rated seven perceived quality indicators of the images online, on a scale of 0 (extremely low quality) to 100 (extremely high quality). A Python-based random forest model was used to train the ratings and the proportions of different landscape elements, enabling automated scoring of the entire street view image dataset. The values of the GSE indicators for each grid were calculated as the average score of all corresponding images within the grid. To avoid bias caused by insufficient street view images, grids with fewer than five observation points (i.e., fewer than 20 images) were excluded. Ultimately, 2,750 grids were included as valid samples for the analysis.

2.3 Socio-Economic Indicators

Studies have shown that population density, per capita GDP, and housing price are closely linked to socio-economic conditions[31]~[33]. Housing price, as an important indicator refecting socio-economic status, has shown reliability and validity in empirical research. For instance, Jinguang Zhang employed housing price as a proxy for household income to analyze spatial and social inequalities in GSE accessibility, availability, and attractiveness in central urban area of Nanjing[34]. Siqi Yu et al. revealed spatial disparities in urban park accessibility among different socio-economic groups in the main urban districts of Nanjing based on housing prices[35]. Accordingly, this research uses housing price as the primary socio-ecnomic indicator in spatial analysis, with population density and per capita GDP included as covariates. Population density was obtained from the 2020 WorldPop database (100 m resolution). Per capita GDP was calculated by dividing 2020 district-level GDP by the registered population, using data from the Statistics Bureau of Nanjing Municipality. Housing price data were collected from online property listing and rental platform—Lianjia. First, ArcGIS 10.3 was adopted to segment and calculate the average population density for each grid; second, the per capita GDP of the administrative district in which each grid is located was assigned to that grid; finally, the average housing price of all residential properties within each grid was calculated.

2.4 Data Analysis

In the ArcGIS 10.3 platform, the natural breaks classification method was used to divide the GSE indicator values, observed at both overhead and eye levels, into seven levels of visualization, aiming to assess the geographical equity of GSE in the study area. For social equity analysis, univariate Moran's I was first used to examine the spatial autocorrelation of housing prices, yielding a value of 0.924 (p = 0.001), indicating a strong and positive spatial autocorrelation in housing price across the study area. Subsequently, a bivariate local Moran's I test and spatial correlation analysis were conducted separately for housing price and GSE indicators, accompanied by visualization. Four regression models were then employed to analyze the relationships between housing price and GSE indicators, including ordinary least squares (OLS) model, spatial lag model (SLM), spatial error model (SEM), and geographically weighted regression (GWR). Population density and per capita GDP were used as covariates. The OLS model is expressed as follows:

$$HP_i = \alpha_0 + \alpha_1 GS_i + \alpha_2 PO_i + \alpha_3 GDP_i + \varepsilon_0 \ , \qquad (2)$$

where HP_i, GS_i, PO_i, and GDP_i represent housing price, GSE indicators, population density, and per capita GDP in the i-th grid, respectively;

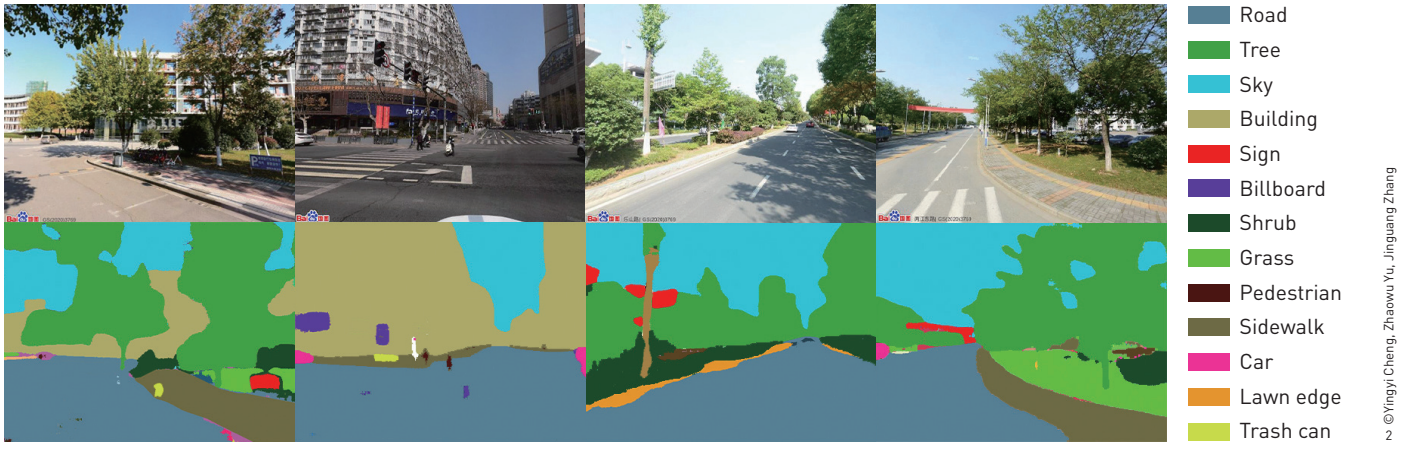

©Yingyi Cheng, Zhaowu Yu, Jinguang Zhang

2. Examples of semantic segmentation results for street view images.

α_0 is the constant term, and ε_0 is the error term.

A spatial autocorrelation test was conducted on the residuals of the OLS model for each GSE indicator. The results showed that all residuals had significantly positive Moran's *I* values (e.g., the Moran's *I* for the residuals of the OLS model with NDVI as the independent variable was 0.878, $p = 0.001$). This indicates that the current OLS model failed to adequately capture the spatial structure in the data. Therefore, based on Eq. (2), spatial regression models (SLM and SEM) were constructed with distance weighting as follows:

$$HP_i = \alpha_0 + \gamma W_i + \alpha_1 GS_i + \alpha_2 PO_i + \alpha_3 GDP_i + \varepsilon_0, \quad (3)$$

where γW_i represents the spatial lag of neighboring regions in SLM and the spatial error in SEM. The spatial weights were constructed using a minimum threshold distance of 864 m, ensuring that each grid had at least one neighboring grid. To test the robustness of the results, sensitivity analysis was performed with a threshold of 1,000 m and weights constructed based on Queen's case and Rook's case adjacency criteria.

Although SLM and SEM account for spatial autocorrelation, they capture only global spatial relationships in the study area. In contrast, the GWR model provides local estimates of regression coefficients for each grid, revealing spatial heterogeneity. Using the spgwr package in RStudio, cross-validation determined an optimal bandwidth of approximately 485 m for the GWR analysis. The GWR model is expressed as follows:

$$HP_i = \alpha_0(u_i, v_i) + \alpha_1(u_i, v_i)GS_i + \alpha_2(u_i, v_i)PO_i + \alpha_3(u_i, v_i)GDP_i + \varepsilon_0, \quad (4)$$

where HP_i, GS_i, PO_i, GDP_i, and ε_0 have the same definitions as in Eq. (2) and Eq. (3). $\alpha_0(\mu_i, v_i)$ represents the intercept for the *i*-th grid, and $\alpha_1(\mu_i, v_i)$, $\alpha_2(\mu_i, v_i)$, and $\alpha_3(\mu_i, v_i)$ are the location-specific regression coefficients, which vary with the geographic coordinates (μ_i, v_i).

The models were then evaluated for goodness of fit using parameters such as the coefficient of determination (R^2) and Akaike information criterion (*AIC*). The GWR model produced spatially varying regression coefficients, which were visualized to reveal the spatial variation of each GSE indicator across the study area. This analysis is instrumental in identifying areas and GSE indicators significantly correlated with housing price, uncovering spatial social heterogeneity in GSE and providing valuable insights for developing scientific and refined grid-based intervention strategies to address blind spots of GSE.

3 Results and Discussion

3.1 Spatial Distribution Characteristics of GSE Indicators

At the overhead level, GSE composition indicators revealed uneven distributions (Fig. 3). NDVI, tree coverage rate, and PLAND showed similar spatial patterns, with lower values in densely built-up central area and higher values near mountains; while peripheral areas generally exhibited higher values than the central area, indicating higher levels of GSE in these areas. Grassland and cropland coverage rate displayed similar spatial patterns, with lower values in the central area and the areas near mountains, and relatively higher values in peripheral areas. For GSE configuration indicators, NP and LPI exhibited contrasting distributions: green spaces in the central area were smaller but more numerous, whereas those in the northeastern and peripheral areas were larger but fewer. ED, SHAPE, FRAC, and COHESION displayed relatively balanced distributions, suggesting that green spaces in the study area had regular shapes and high aggregation.

At the eye level, the quantity and perceived quality also exhibited uneven spatial distributions (Fig. 4). *GVI*, vegetation abundance, and openness showed spatial patterns similar to NDVI, with higher values in peripheral areas compared with densely built-up central areas, reflecting better greenery and more open streetscapes. Walkability, accessibility, amenity, neatness, and safety exhibited similar patterns, with generally high values, indicating sound overall quality of street environments in the study area.

3.2 Spatial Correlation Between GSE Indicators and Housing Price

In the study area, the housing prices were the highest in the cultural core of ancient capital and Hexi Area, gradually decreasing outwards (Fig. 5). The bivariate local Moran's *I* results (Fig. 6) showed that the larger the absolute value of the Moran's *I*, the stronger the spatial correlation between GSE indicators and housing price. Results indicated significant spatial correlations between housing price and all 19 GSE indicators. Notably, grassland coverage rate, cropland coverage rate, NP, and vegetation abundance showed negative spatial correlations with housing price. This suggests that better green space conditions (e.g., dominated by trees with high quantity and quality), larger area, greater shape diversity, and higher cohesion were associated with higher housing price. Furthermore, the absolute value of Moran's *I* for housing price and overhead GSE indicators were generally lower than those for housing price and eye-level GSE indicators. Among them, tree coverage rate and cropland coverage rate had relatively higher absolute Moran's *I* of 0.129 and 0.171, respectively. For eye-level indicators, amenity,

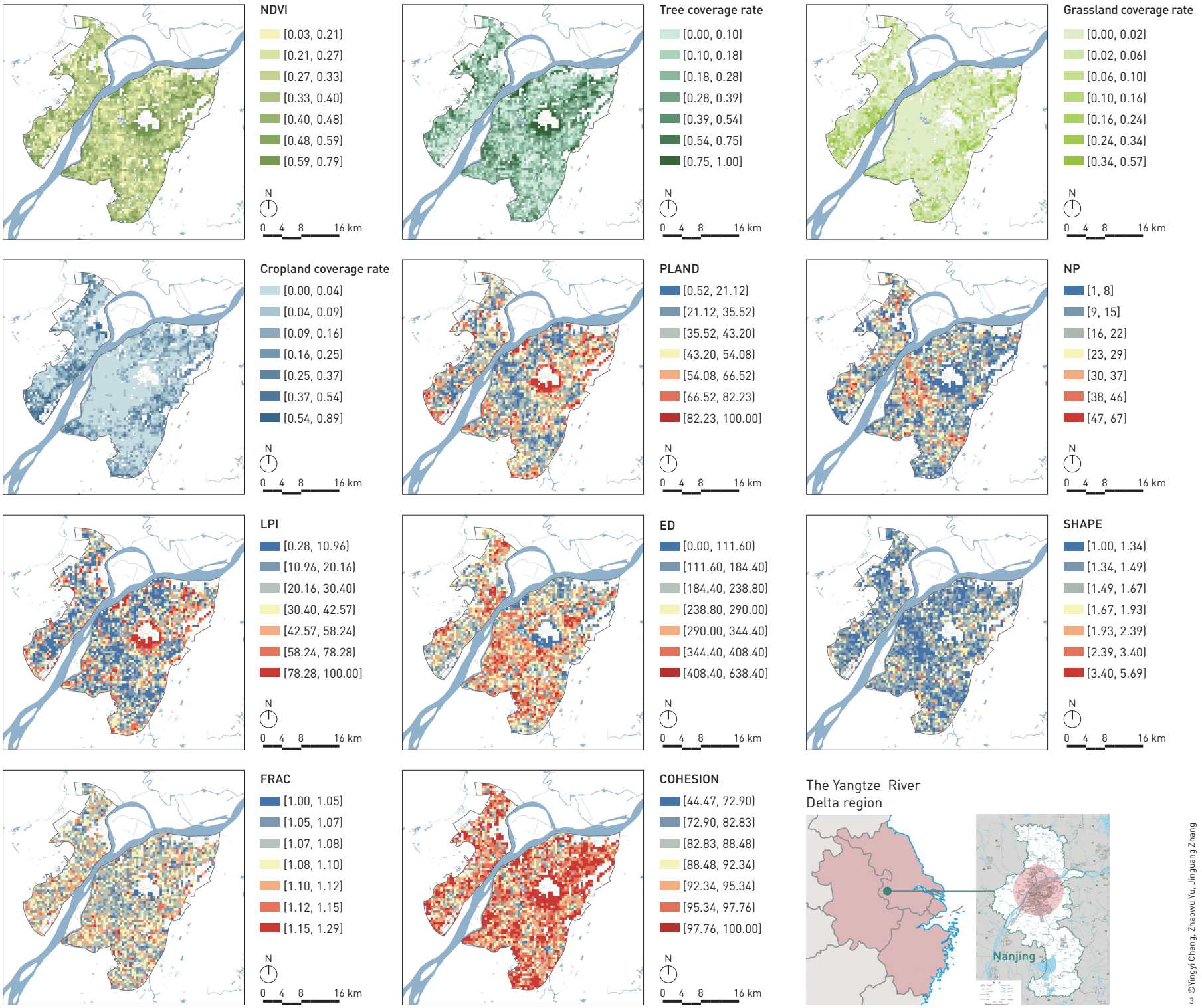

3. The spatial distribution of GSE indicators at the overhead level.

neatness, and accessibility showed higher absolute Moran's *I* of 0.292, 0.254, and 0.232, respectively. These findings suggest that housing price is closely associated with both quantity and perceived quality, aligning with the results of previous studies exploring the relationship between urban green space and housing price[36][37].

Table 3 presents the regression analysis results of the four models for different GSE indicators at both overhead and eye levels. Overall, the spatial regression models (SLM, SEM, and GWR) greatly outperformed the OLS model in terms of goodness of fit, with SLM and SEM achieving the best results, followed by GWR. Sensitivity

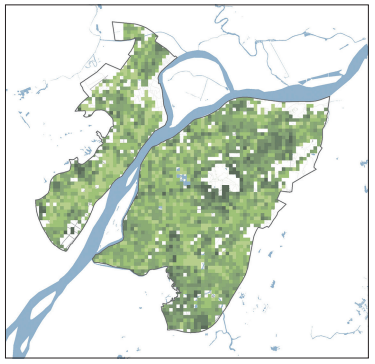

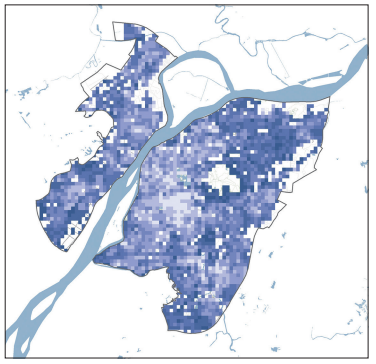

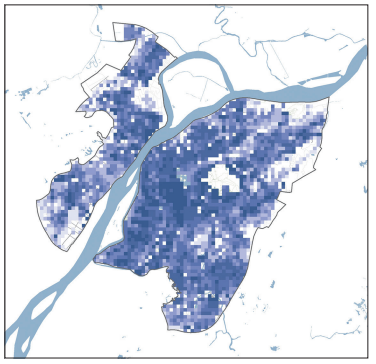

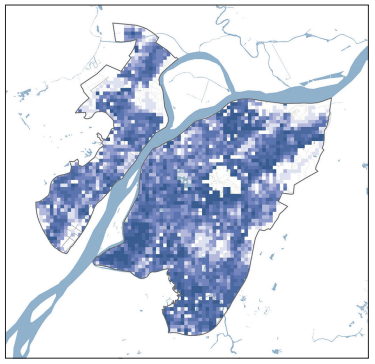

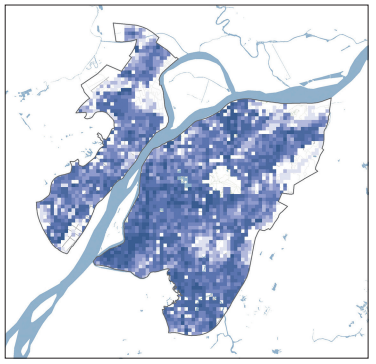

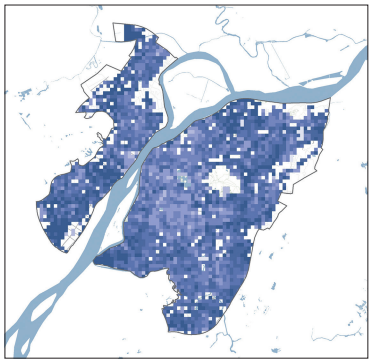

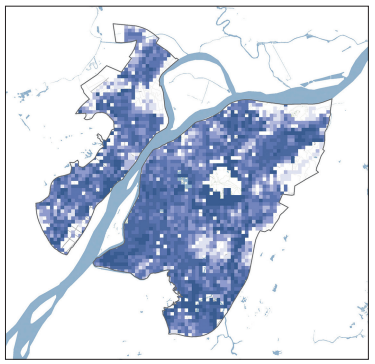

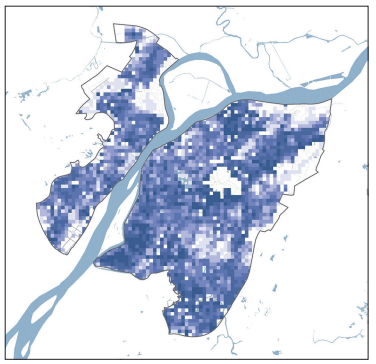

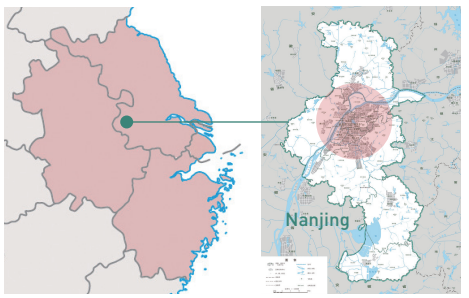

©Yingyi Cheng, Zhaowu Yu, Jinguang Zhang

4. The spatial distribution of GSE indicators at the eye level.
5. The spatial distribution of housing price in study area.
6. The spatial correlation between housing price and different GSE indicators.

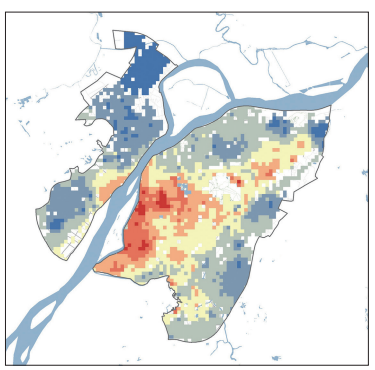

©Yingyi Cheng, Zhaowu Yu, Jinguang Zhang

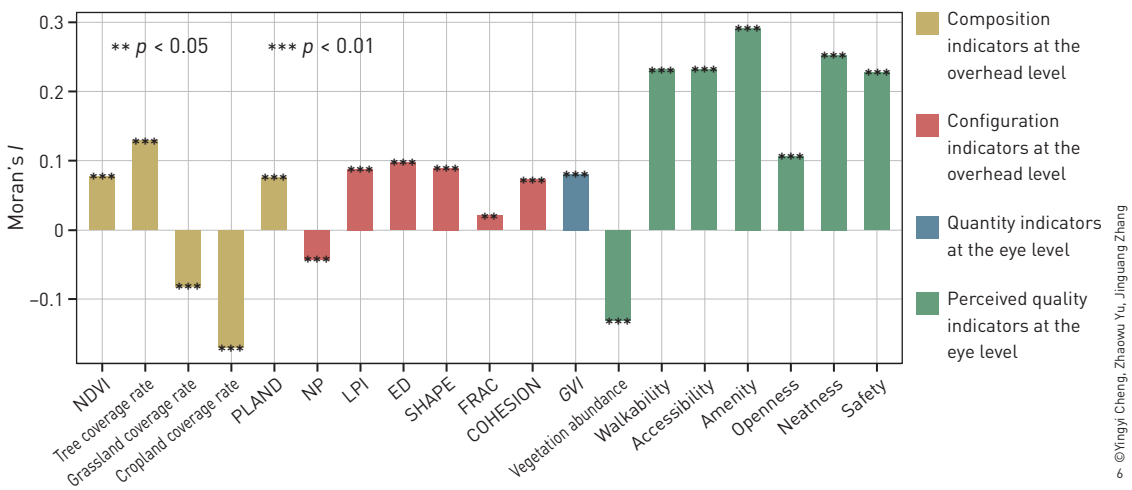

©Yingyi Cheng, Zhaowu Yu, Jinguang Zhang

Table 3: Fitting results of the housing price with GSE indicators at the overhead and eye levels

Variable	OLS			SLM			SEM			GWR	
	R^2	*AIC*	Log likelihood	R^2	*AIC*	Log likelihood	R^2	*AIC*	Log likelihood	R^2	*AIC*
Overhead level											
NDVI	0.131	−3,948.410	1,978.210	0.939	−10,480.800	5,245.420	0.939	−10,477.500	5,242.766	0.903	−9,688.662
Tree coverage rate	0.136	−3,964.150	1,986.070	0.939	−10,481.700	5,245.830	0.939	−10,477.000	5,242.495	0.903	−9,696.385
Grassland coverage rate	0.107	−3,872.520	1,940.260	0.938	−10,457.700	5,233.830	0.938	−10,459.700	5,233.833	0.905	−9,735.061
Cropland coverage rate	0.111	−3,885.630	1,946.820	0.938	−10,458.200	5,234.100	0.939	−10,461.800	5,234.890	0.904	−9,705.012
PLAND	0.135	−3,960.390	1,984.200	0.939	−10,492.000	5,251.000	0.939	−10,485.200	5,246.622	0.904	−9,699.222
NP	0.139	−3,973.290	1,990.840	0.940	−10,524.300	5,267.600	0.939	−10,506.100	5,257.050	0.905	−9,742.258
LPI	0.136	−3,965.890	1,986.950	0.939	−10,498.000	5,254.010	0.939	−10490.000	5,248.996	0.905	−9,716.672
ED	0.108	−3,876.800	1,942.400	0.938	−10,459.800	5,234.920	0.939	−10,462.700	5,235.339	0.901	−9,641.370
SHAPE	0.129	−3,942.570	1,975.280	0.939	−10,495.000	5,252.510	0.939	−10,476.300	5,242.135	0.903	−9,960.407
FRAC	0.111	−3,886.590	1,947.290	0.939	−10,465.600	5,237.820	0.939	−10,462.200	5,235.102	0.898	−9,528.610
COHESION	0.130	−3,946.140	1,977.070	0.939	−10,512.700	5,261.350	0.939	−10,501.800	5,254.885	0.604	−6,100.009
Eye level											
GVI	0.125	−3,930.530	1,969.260	0.939	−10,471.400	5,240.720	0.939	−10,469.900	5,238.950	0.902	−9,655.261
Vegetation abundance	0.107	−3,873.060	1,940.530	0.939	−10,465.800	5,237.910	0.939	−10,474.500	5,241.269	0.862	−8,877.027
Walkability	0.126	−3,931.390	1,969.690	0.938	−10,458.300	5,234.140	0.938	−10,459.400	5,233.694	0.895	−9,514.691
Accessibility	0.153	−4,016.13	2,012.060	0.938	−10,457.100	5,233.540	0.938	−10,454.600	5,231.292	0.881	−9,235.790
Amenity	0.173	−4,083.690	2,045.850	0.938	−10,460.200	5,235.110	0.938	−10,454.800	5,231.394	0.889	−9,090.944
Openness	0.109	−3,836.550	1,922.280	0.938	−10,354.400	5,182.220	0.938	−10,357.200	5,182.623	0.864	−8,838.506
Neatness	0.162	−4,049.470	2,028.740	0.938	−10,464.700	5,237.370	0.938	−10,459.700	5,233.835	0.846	−8,614.218
Safety	0.152	−3,971.400	1,989.700	0.938	−10,359.600	5,184.820	0.938	−10,357.300	5,182.643	0.872	−9,062.314

NOTE
The R^2 of the GWR model for all GSE indicators in this table is the global mean value and there is no log likelihood term.

analysis using different weighting schemes confirmed the robustness of the findings, as SLM and SEM results were consistent with those reported in Table 3, with R^2 values exceeding 0.9. It validated the robustness of the findings and reaffirmed the significant spatial correlation between GSE indicators and housing price.

3.3 Spatial Association and Heterogeneity Between GSE Indicators and Housing Price

The coefficient estimation results (Figs. 7, 8) showed that the estimated coefficients for all the GSE indicators in the study area simultaneously had both positive and negative values, with

7. Coefficient estimations of housing price and GSE indicators at the overhead level.

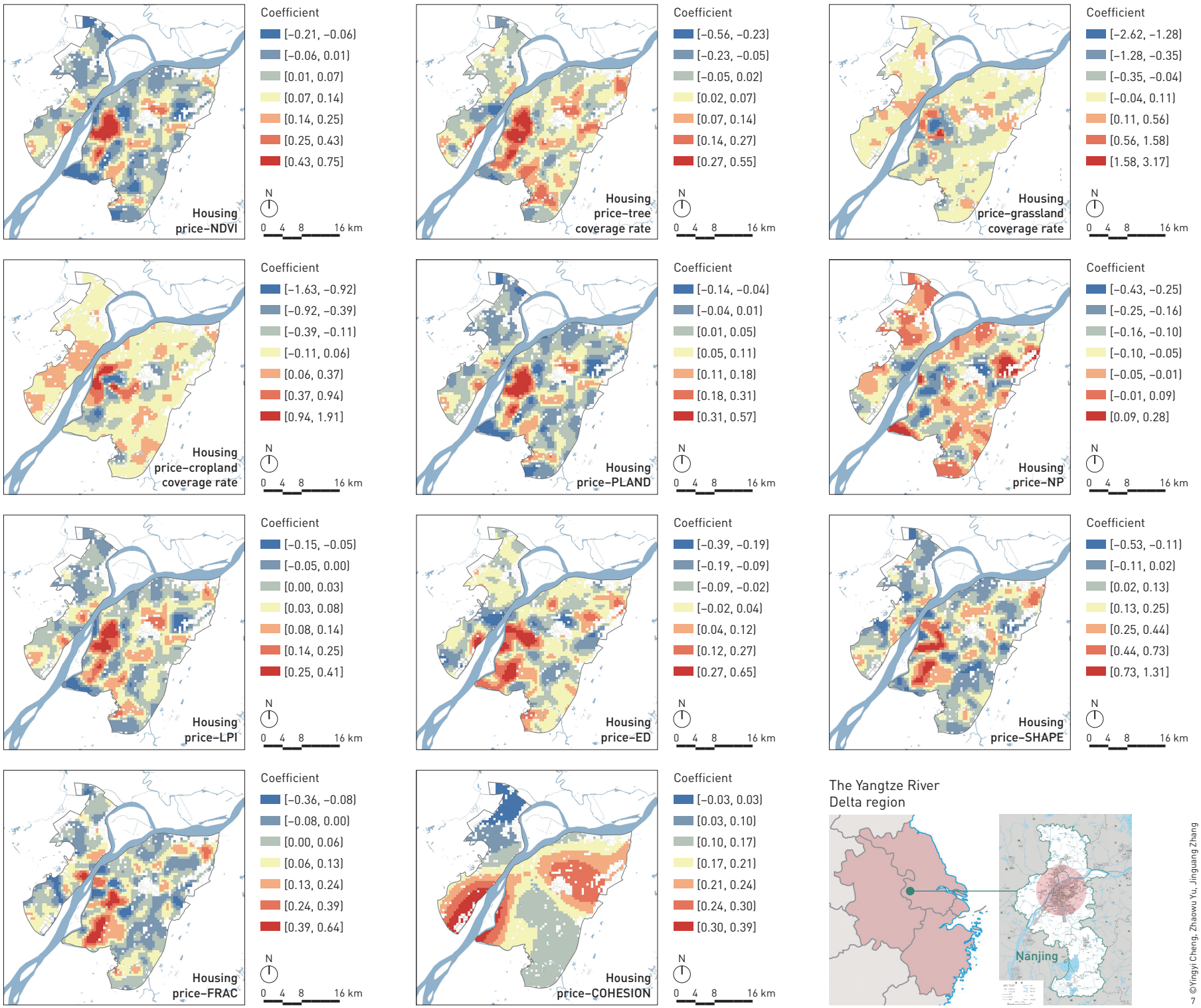

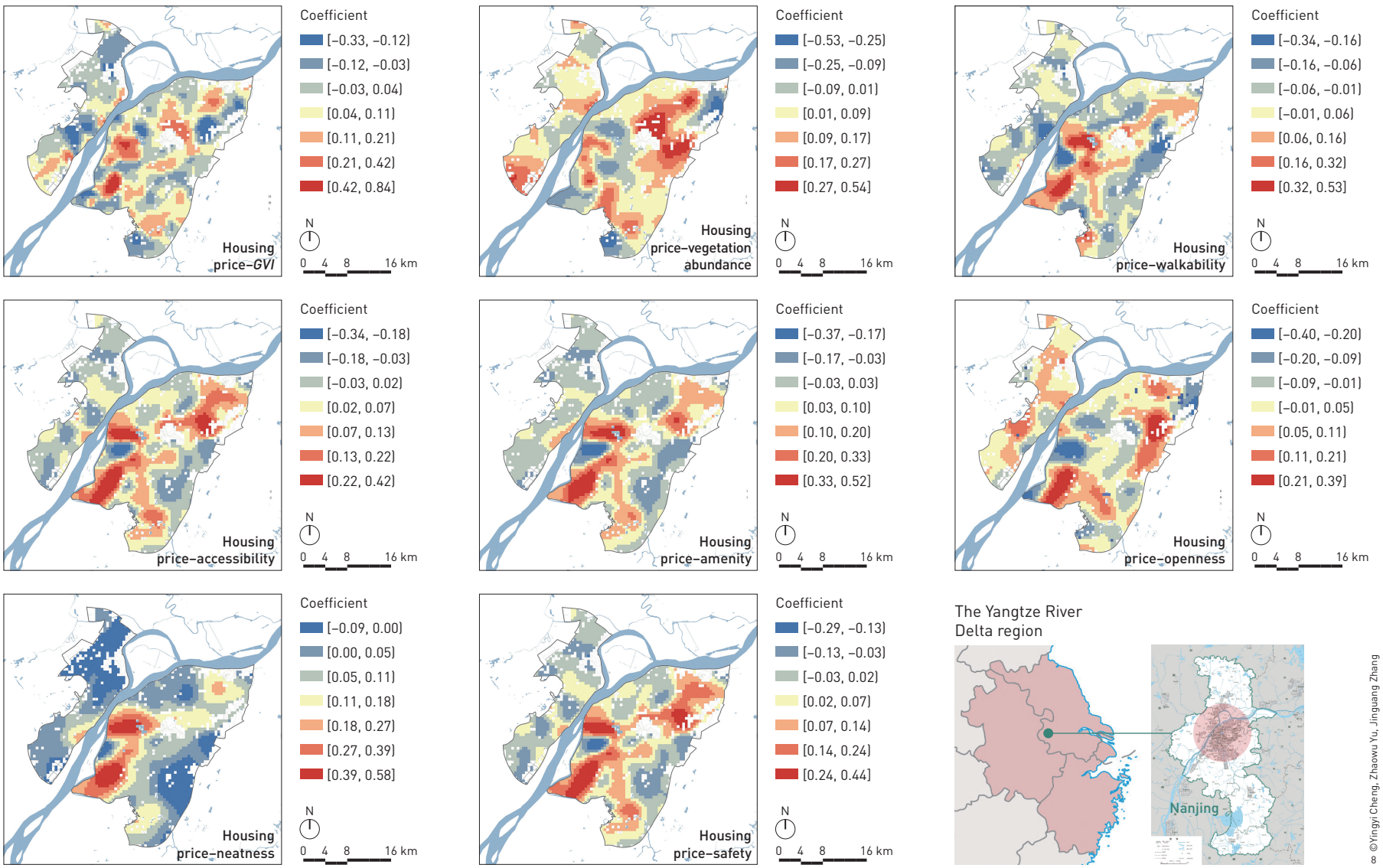

8. Coefficient estimations of housing price and GSE indicators at the eye level.

a notable proportion of negative values, suggesting significant social equity heterogeneity of GSE. According to the distribution of housing price (Fig. 5), high-price areas exhibited positive coefficients for NDVI, tree coverage rate, PLAND, LPI, ED, and SHAPE at the overhead level, indicating that in these areas, as vegetation coverage increases, green space size grows, the diversity of green space shapes increases, and the connectivity with the surrounding environment improves, housing price tends to rise. Similarly, in high-price areas, the estimated positive coefficients for *GVI*, walkability, accessibility, amenity, neatness, and safety at the eye level indicated that as quantity and the quality of the street green space improve, housing price also increases. Conversely, in low-price areas, the coefficients for these indicators were estimated as negative, implying that GSE and housing price were negatively correlated. This result may be influenced by the geographical locations of these areas, which are typically on the periphery of the central city, where green space conditions are relatively good. Therefore, rather than an increase in GSE, urbanization levels may play a more significant role in raising housing prices in these areas. The relationship between the quantity and quality of street green spaces and housing price has also been confirmed in previous studies. Zhaocheng Bai et al. revealed a positive correlation between quantity of street green spaces and housing price in the central urban area of Hangzhou, China[38]. Ying Li et al. found that street quality characteristics could influence housing price by as much as 36.74% in Guangzhou, China[39]. Furthermore, in most high-price areas

in this research, the coefficients for grassland coverage rate, cropland coverage rate, NP, vegetation abundance, and openness were negative, indicating that subareas with lower building density and urbanization levels tend to have relatively lower housing prices in high-price areas.

3.4 Planning Intervention Strategies for GSE

Based on the above analysis, this research found that GSE indicators at the eye level exhibit a stronger spatial correlation with socio-economic status than those at the overhead level. Therefore, planning strategies aimed at promoting "green equity" should prioritize enhancing the quantity and quality of street green spaces. At the micro scale, this research identified low-GSE zones requiring optimization by analyzing the heterogeneity of geographical and social equity of GSE indicators, and proposed targeted optimization strategies for high and low socio-economic areas① within these zones.

1) Low-GSE, high socio-economic status zones. In these zones, GSE and socio-economic status are negatively correlated, typically characterized by high housing prices but limited green spaces with small, regular shape, and poor overall vegetation coverage. Such sites are often found in well-developed areas with relatively high living standards. The scarcity of available land makes it challenging to increase the amount of green spaces. Thus, structural adjustments to existing ones, such as improving shapes of green spaces to enhance residents' access, could be considered. The more complex the green patch shapes, the higher the coupling between green space boundaries and the surrounding environment, which can provide more accesses for residents to interact with green spaces. Additionally, green corridors can be created along linear spaces like roads and rivers to connect fragmented green spaces and improve overall GSE levels in urban areas.

2) Low-GSE, low socio-economic status zones. In these zones, GSE and socio-economic status are positively correlated. Such zones are typically located on the periphery of the study area, with lower housing price and urban vitality, and also have higher proportions of grassland and cropland compared with tree coverage. As indicated earlier, grassland and cropland coverage rates exhibit negative spatial correlations with socio-economic status, while tree coverage rate exhibits a positive correlation. Therefore, the focus of increasing green spaces in such areas should be on encouraging tree planting. The addition of trees and shrubs to grassland areas could enhance the visual layering of the landscape while improving the quality of GSE.

① High/low socio-economic status zones were defined based on the spatial distribution of housing price shown in Fig. 4, where color yellow represents the intermediate level, deeper blue indicates lower socio-economic status, and deeper red indicates higher levels.

4 Conclusions and Prospects

This research developed a comprehensive urban GSE assessment model at both overhead and eye levels. Using housing price as a proxy for residents' socio-economic status, this research adopted OLS, SLM, and SEM models to evaluate the geographical and social equity of GSE in Nanjing's central urban area. To conduct a more detailed spatial heterogeneity analysis of GSE's social equity, GWR model was employed to visualize grid-level spatial correlations between GSE and housing prices.

The results revealed an uneven distribution of GSE across the study area. Green spaces in the central area were fragmented, and overall GSE was lower than peripheral areas. A significant spatial correlation was observed between housing price and GSE indicators, with eye-level GSE indicators exhibiting stronger correlations with housing price than overhead-level indicators. Grassland coverage rate, cropland coverage rate, NP, and vegetation abundance showed negative correlations with housing price, while all other GSE indicators displayed positive correlations. Additionally, SLM and SEM models demonstrated the best predictive performance for housing price based on GSE indicators. The GWR model further showed significant imbalances in both geographical and social equity of GSE within the central urban area of Nanjing.

This research identified urban areas with insufficient GSE and proposed targeted planning interventions separately for low-GSE, high socio-economic status zones, and low-GSE, low socio-economic status zones. Theoretically, the research extends the empirical application of Exposure Ecology studies. Practically, it provides actionable insights for advancing urban GSE assessments and offers guidance for promoting equity in GSE through urban planning and green space system design.

This study has several limitations. First, differences in the number, profession, and age distribution of volunteers scoring street-view image training sets might introduce bias in perceived quality evaluations. Future studies should control these factors to improve robustness of the results. Second, using community housing price as a proxy for socio-economic status has certain constrains. Future research could incorporate

additional indicators, such as average household income and education levels, for a more comprehensive assessment. Third, the analysis results based on cross-sectional data cannot reveal causal relationships between GSE and housing price. Future research can use long time-series data to fill this gap. Lastly, the sample selection from high-density urban areas may limit the generalizability of the planning strategies. Future research should explore the heterogeneity of GSE equity in a multi-scale, multi-temporal, and cross-regional context.

Competing interests | The authors declare that they have no competing interests.

REFERENCES

[1] Yu, Z., Yang, G., Zuo, S., Jørgensen, G., Koga, M., & Vejre, H. (2020). Critical review on the cooling effect of urban blue-green space: A threshold-size perspective. *Urban Forestry & Urban Greening*, (49), 126630.

[2] Yao, X., Yu, Z., Ma, W., Xiong, J., & Yang, G. (2024). Quantifying threshold effects of physiological health benefits in greenspace exposure. *Landscape and Urban Planning*, (241), 104917.

[3] Li, M., Wen, Y., & Hu, G. (2024). Research status of urban greenspace exposure and public health relation. *Journal of Zhejiang Sci-Tech University (Natural Sciences)*, 51(4), 492–506.

[4] Lin, T., Zeng, Z., Yao, X., Geng, H., Yu, Z., Wang, L., Lin M., Zhang, J., & Zheng, Y. (2023). Research of urban green space exposure and its effects on human health. *Acta Ecologica Sinica*, 43(23), 10013–10021.

[5] Wu, J., Si, M., & Li, W. (2016). Spatial equity analysis of urban green space from the perspective of balance between supply and demand: A case study of Futian District, Shenzhen, China. *Chinese Journal of Applied Ecology*, 27(9), 2831–2838.

[6] Heo, S., & Bell, M. L. (2023). Investigation on urban greenspace in relation to sociodemographic factors and health inequity based on different greenspace metrics in 3 US urban communities. *Journal of Exposure Science & Environmental Epidemiology*, 33(2), 218–228.

[7] Markevych, I., Schoierer, J., Hartig, T., Chudnovsky, A., Hystad, P., Dzhambov, A. M., de Vries, S., Triguero-Mas, M., Brauer, M., Nieuwenhuijsen, M. J., Lupp, G., Richardson, E. A., Astell-Burt, T., Dimitrova, D., Feng, X., Sadeh, M., Standl, M., Heinrich, J., & Fuertes, E. (2017). Exploring pathways linking greenspace to health: Theoretical and methodological guidance. *Environmental Research*, (158), 301–317.

[8] Zhang, J., Yu, Z., Zhao, B., Sun, R., & Vejre, H. (2020). Links between green space and public health: A bibliometric review of global research trends and future prospects from 1901 to 2019. *Environmental Research Letters*, 15(6), 063001.

[9] Wheeler, B. W., Lovell, R., Higgins, S. L., White, M. P., Alcock, I., Osborne, N. J., Husk, K., Sabel, C. E., & Depledge, M. H. (2015). Beyond greenspace: An ecological study of population general health and indicators of natural environment type and quality. *International Journal of Health Geographics*, (14), 1–17.

[10] Yang, G., Yu, Z., Zhang, J., Liu, H., Jin, G., Ju, Y., Hong, B., Zhao, H., Zhang, L., Yao, X., Ma, W., Xiong, J., Shao, Y., & Jiang, B. (2024). Research progress and prospects on the health benefits of greenspace exposure from the perspective of exposure ecology. *Acta Ecologica Sinica*, 44(14), 5914–5924.

[11] Astell-Burt, T., Walsan, R., Davis, W., & Feng, X. (2023). What types of green space disrupt a lonelygenic environment? A cohort study. *Social Psychiatry and Psychiatric Epidemiology*, 58(5), 745–755.

[12] Zhang, J., Song, A., Xia, T., & Zhao, B. (2023). Evaluating the urban park green space exposure from the perspective of the community life circle. *Journal of Nanjing Forestry University (Natural Sciences Edition)*, 47(3), 191–198.

[13] Gonzales-Inca, C., Pentti, J., Stenholm, S., Suominen, S., Vahtera, J.,

& Käyhkö, N. (2022). Residential greenness and risks of depression: Longitudinal associations with different greenness indicators and spatial scales in a Finnish population cohort. *Health & Place*, (74), 102760.

[14] Grafius, D. R., Corstanje, R., & Harris, J. A. (2018). Linking ecosystem services, urban form and green space configuration using multivariate landscape metric analysis. *Landscape Ecology*, (33), 557–573.

[15] Sheng, S., & Wang, Y. (2024). Configuration characteristics of green-blue spaces for efficient cooling in urban environments. *Sustainable Cities and Society*, (100), 105040.

[16] Wang, R., Feng, Z., Pearce, J., Zhou, S., Zhang, L., & Liu, Y. (2021). Dynamic greenspace exposure and residents' mental health in Guangzhou, China: From over-head to eye-level perspective, from quantity to quality. *Landscape and Urban Planning*, (215), 104230.

[17] Huang, W., Wang, R., Liu, F., Huang, W., Dong, G., & Yu, H. (2022). Association between street view greenness and allergic rhinitis in children. *Journal of Environmental and Occupational Medic*, 39(1), 17–22.

[18] Reyes-Riveros, R., Altamirano, A., De La Barrera, F., Rozas-Vásquez, D., Vieli, L., & Meli, P. (2021). Linking public urban green spaces and human well-being: A systematic review. *Urban Forestry & Urban Greening*, (61), 127105.

[19] Wolch, J. R., Byrne, J., & Newell, J. P. (2014). Urban green space, public health, and environmental justice: The challenge of making cities 'just green enough'. *Landscape and Urban Planning*, (125), 234–244.

[20] Chen, B., & Webster, C. (2022). Eight reflections on quantitative studies of urban green space: A mapping-monitoring-modeling-management (4M) perspective. *Landscape Architecture Frontiers*, 10(3), 66–76.

[21] Yu, Z., Yang, G., Lin, T., Zhao, B., Xu, Y., Yao, X., Ma, W., Vejre, H., & Jiang, B. (2024). Exposure ecology drives a unified understanding of the nexus of (urban) natural ecosystem, ecological exposure, and health. *Ecosystem Health and Sustainability*, (10), 0165.

[22] Zhou, M., & Wang, L. (2023). Change of park green space social equity and its driving forces—From the perspective of population aging. *Chinese Landscape Architecture*, 39(2), 57–63.

[23] Yang, L., Yang, P., & Chen, L. (2020). Quantitative evaluation on the equity of park green space provision: A case study of central district of Chongqing. *Chinese Landscape Architecture*, 36(1), 108–112.

[24] Kabisch, N., & Haase, D. (2014). Green justice or just green? Provision of urban green spaces in Berlin, Germany. *Landscape and Urban Planning*, (122), 129–139.

[25] Mu, H., Gao, Y., Wang, Z., & Zhang, Y. (2019). Equity evaluation of park green space service level from the perspective of supply and demand balance: An empirical analysis based on big data. *Urban Development Studies*, 26(11), 10–15.

[26] Yan, L., Jin, X., & Zhang, J. (2024). Equity in park green spaces: A bibliometric analysis and systematic literature review from 2014–2023. *Frontiers in Environmental Science*, (12), 1374973.

[27] Mitchell, R., & Popham, F. (2008). Effect of exposure to natural environment on health inequalities: An observational population study. *The Lancet*, 372(9650), 1655–1660.

[28] United Nations. (n.d.). *Sustainable development goals—Goal 11: Make cities inclusive, safe, resilient and sustainable*.

[29] Geng, X., Yu, Z., Zhang, D., Li, C., Yuan, Y., & Wang, X. (2022). The influence of local background climate on the dominant factors and threshold-size of the cooling effect of urban parks. *Science of the Total Environment*, (823), 153806.

[30] Statistics Bureau of Nanjing Municipality. (2023). *Nanjing 2022 national economic and social development statistical bulletin*.

[31] Dong, Z., Hui, E. C. M., & Jia, S. (2017). How does housing price affect consumption in China: Wealth effect or substitution effect?. *Cities*, (64), 1–8.

[32] Yegorov, Y. A. (2009). Socio-economic influences of population density. *Chinese Business Review*, 8(7), 1–12.

[33] Wang, T., & Sun, F. (2022). Global gridded GDP data set consistent with the shared socioeconomic pathways. *Scientific Data*, 9(1), 221.

[34] Zhang, J. (2023). Inequalities in the quality and proximity of green space exposure are more pronounced than in quantity aspect: Evidence from a rapidly urbanizing Chinese city. *Urban Forestry & Urban Greening*, (79), 127811.

[35] Yu, S., Zhu, X., & He, Q. (2020). An assessment of urban park access using house-level data in urban China: Through the lens of social equity. *International Journal of Environmental Research and Public Health*, 17(7), 2349.

[36] Liu, Q., Gu, D., Liu, Y., & Lin, X. (2021). The impact of urban landscapes on housing prices in Yuzhong District, Chongqing. *Modern Urban Research*, 36(12), 109–115.

[37] Cui, X., & Fan, L. (2023). Correlation between park green space and housing price in Chengdu City based on landscape index analysis. *Journal of Chinese Urban Forestry*, 21(3), 68–73.

[38] Bai, Z., Qi, J., & Tang, X. (2023). Social differentiation of urban street green quantity: A case study through the lens of visual landscape. *Journal of Tianjin Normal University (Natural Science Edition)*, 43(1), 60–66.

[39] Li, Y., Wang, N., Tong, Z., Liu, Y., An, R., & Liu, Y. (2023). The nonlinear influence of street quality on housing prices based on random forest model: A case study of Guangzhou. *Tropical Geography*, 43(8), 1547–1562.

https://doi.org/10.15302/J-LAF-0-020031 收稿日期 | 2023-12-27 录用日期 | 2024-06-07 中图分类号 | TU984 文献标识码 | A

鸟瞰–目视视角下城市绿地暴露的地理和社会公平性分异研究

承颖怡[1]，余兆武[2,*]，张金光[1]

1 南京林业大学风景园林学院，南京 210037
2 复旦大学环境科学与工程系，上海 200438

*通讯作者
地址：上海市杨浦区邯郸路220号
邮编：200438
邮箱：zhaowu_yu@fudan.edu.cn

图文摘要

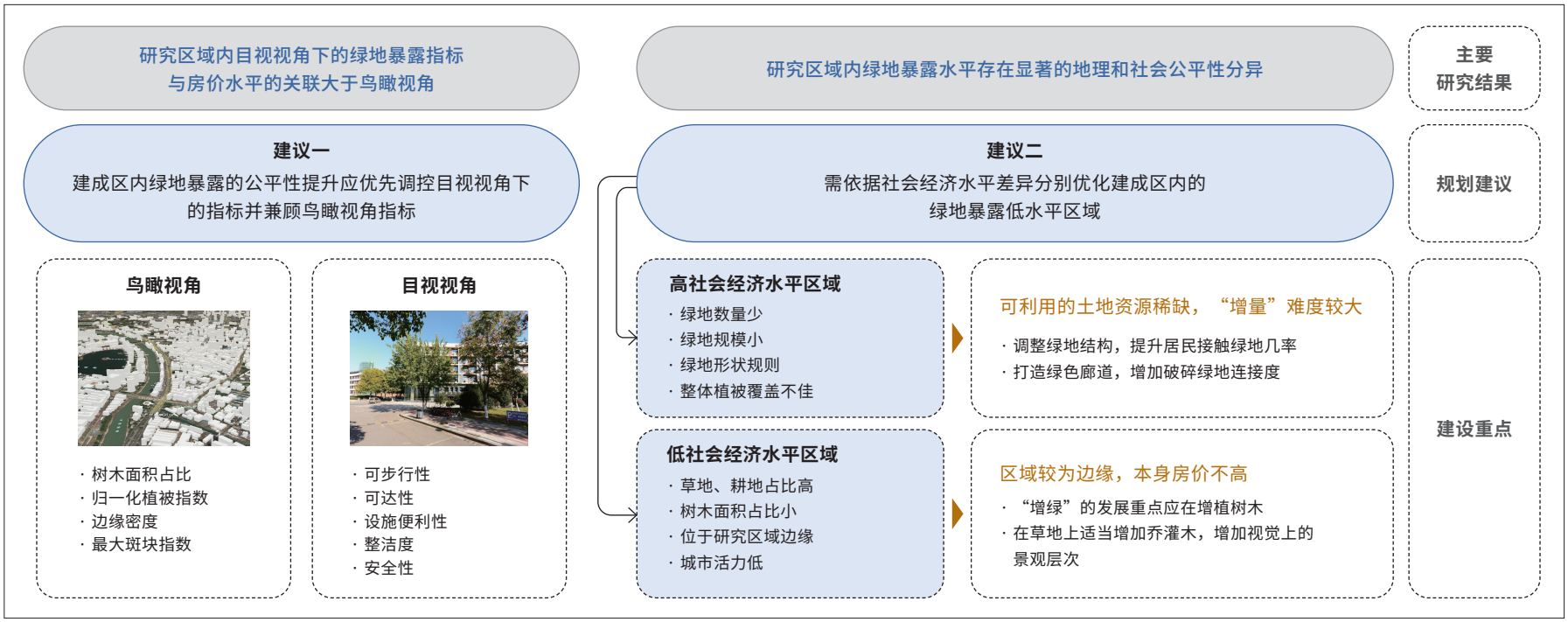

摘要

提升绿地暴露水平是上游主动式干预公众健康的重要抓手。然而，绿地在城市空间中常呈现不均衡分布，引发了针对“绿色公平”等议题的讨论。本研究旨在基于鸟瞰–目视视角系统地评估绿地暴露水平，剖析绿地暴露的地理–社会公平性分异并提出规划调控策略。本文以南京市中心城区为研究区域，首先从鸟瞰视角下的绿地组成和配置及目视视角下的绿量和街景感知质量构建绿地暴露评估体系，评估绿地暴露的地理公平性。其次，选取房价作为社会经济指标，使用空间回归模型分析绿地暴露与房价水平的空间关联，评估绿地暴露的社会公平性。研究发现：1）研究区域内绿地暴露在地理公平性和社会公平性层面均存在显著失衡现象；2）目视视角下的绿地暴露指标与房价水平的空间自相关性为0.08～0.29，普遍高于鸟瞰视角（0.02～0.13）；3）绿地暴露与房价的空间关联存在显著分异特征，高房价群体更易享受绿地服务。研究成果精准识别了绿地暴露盲区，以及绿地供给与社会经济水平的失衡区域，为科学“增绿”提供了有效指引，也可以进一步促进暴露生态学理论的实证研究。

关键词

暴露生态学；绿地暴露；城市绿地；地理公平；社会公平；空间回归模型

文章亮点

- 构建了涵盖鸟瞰－目视视角指标的城市绿地暴露综合评估框架
- 使用四种空间回归模型评估了城市绿地暴露的社会公平性
- 房价水平与鸟瞰－目视视角下的绿地暴露指标均存在显著空间关联
- 依据地理加权模型结果为具有不同绿地暴露现状的区域提供了优化策略

基金项目

- 国家自然科学基金面上项目“城市绿地热缓解效率阈值多尺度耦合研究”（编号：42171093）
- 国家自然科学基金青年基金项目“融合多样化需求的城市居住区公共服务设施空间配置水平与机制研究”（编号：42201200）
- 国家自然科学基金青年基金项目“城市人群绿地暴露生理健康效应阈值测度及影响因素研究”（编号：42401103）
- 上海市“科技创新行动计划”自然科学基金项目“多尺度下城市绿色植被对热环境缓解研究”（编号：21ZR1408500）
- 上海市浦江学者人才计划项目“典型气候背景下城市绿地降温效率阈值与能量动态机理研究”（编号：21PJ1401600）
- 江苏省高校自然科学基金面上项目“面向健康城市的绿色空间暴露水平系统性测度与优化配置研究”（编号：22KJB220006）

编辑 高雨婷，马锡栋
翻译 高雨婷

1 引言

绿地作为城市中重要的生态空间，是建设生态韧性城市、提升居民生活品质的重要自然资源[1][2]。它不仅为城市提供了广泛的生态系统服务，也是居民亲近和感受自然的重要场所[3][4]。然而，在城市空间中，尤其是高密度城市区域，绿地是一种稀缺的自然资源，且常常呈现不均衡分布，引发了一系列公平性问题[5][6]。

绿地暴露（green space exposure，GSE）是指居民与城市绿地直接或间接的接触与互动[7]。居民能够充分暴露于城市绿地中是实现绿地健康促进效益的先决条件[8]。近年来，国内外学者广泛研究了城市GSE特征，包括对绿地空间格局及其健康效应的测度[9][10]。现有研究所涉GSE评价指标主要集中在鸟瞰视角，如绿地面积、归一化植被指数、树冠覆盖率和植被覆盖率[11]~[13]；亦有部分研究评估了城市绿地的景观结构等配置特征，如破碎程度、形状复杂性和斑块凝聚度等[14][15]。然而，此类研究大多基于卫星图像数据揭示大范围GSE的时空特征，无法测量垂直维度的GSE及居民在时空行为中与城市绿地的实际接触情况，因此难以反映GSE的内在复杂性、多样性和动态性。随着大数据与机器学习技术的普及应用，有学者初步探索了目视视角下的城市GSE指标研究，如利用街景图像测量绿视率并量化街道空间质量[16][17]。尽管现有研究已逐渐从单一维度的GSE评估转变为多维度评估[9][18][19]，但仍缺乏系统的城市GSE评估模型。陈斌等学者也强调了在城市绿地量化研究中综合考虑绿地数量、质量、类型和结构属性的重要性，并提出测量GSE应考虑空间、时间和社会差异[20]。在理论层面，余兆武等人进一步提出了暴露生态学理论体系来系统理解（城市）自然生态系统、生态暴露与健康之间的耦合关系[21]。城市GSE的地理和社会公平性相关研究是暴露生态学理论下“客体－现实”维度的重要研究内容。

绿地公平性研究经历了从数量公平到空间公平再到社会公平的嬗变[22]。过去研究多采用传统绿地覆盖指标（如绿地率、人均绿地面积）衡量绿地在行政区划内的服务能力。尽管此类指标能够揭示供给情况，但较难反映人口－绿地的供需关系[20][23]。随着研究的深入，将人口分布和社会经济属性纳入考量的GSE社会公平性研究逐渐成为热点[24][25]。研究表明，GSE公平性在不同地理区域、具有不同文化和发展历史的地区存在差异[26]。GSE不平等也可能导致公众健康不平等，而这种负面影响在社会经济水平低下的人群中更为明显[27]。联合国可持续发展目标提出要“向所有人，特别是妇女、儿童、老年人和残障人群，普遍提供安全、包容、无障碍、绿色的公共空间”的目标[28]。系统地评估城市GSE水平并识别其盲区，厘清其在地理和社会维度的公平性分异特征并提出规划干预策略，是实现科学“增绿”的重要途径，也是上游主动式干预公众健康的重要抓手[29]。然而，现有研究缺乏对高密度城市区域中GSE的地理公平性与社会公平性的全面评估，难以为不同GSE现状的区域

提供优化策略。

综上，本研究在暴露生态学视角下，旨在构建鸟瞰－目视视角下城市GSE评估体系，系统性地衡量城市GSE地理和社会公平性，拟回应以下科学问题：1）鸟瞰－目视视角下城市GSE空间分布特征是什么？2）城市GSE和房价水平是否存在空间关联及空间异质性？

2 研究方法

2.1 研究区域

本研究选取中国南京市中心城区为研究区域（图1）。截至2022年末，南京市总人口约为950万，其中城镇人口约826万[30]。依据《南京国土空间总体规划（2021—2035）》，中心城区包含新街口、河西、城南和江北四个市级中心，总体规划范围为804km^2。中心城区不仅经济繁荣，还覆盖了古都文化核，在文化和历史方面具有重要地位，同时也是人口密度最高、路网最为复杂的区域。本研究利用ArcGIS 10.3将其划分为500m × 500m的渔网网格，并以单个网格作为研究样本。

2.2 城市GSE评估模型构建

本研究从鸟瞰－目视视角构建城市GSE评估体系。其中，鸟瞰视角包括城市绿地的组成和配置两类指标，目视视角包括绿量及街景感知质量两类指标（表1，2）。

2.2.1 鸟瞰视角下的城市GSE指标选取及数据获取

研究首先从哥白尼开放获取中心网站下载2021年9月的哨兵–2号卫星影像（分辨率为10m），经哨兵数据应用平台（SNAP）及ArcGIS 10.3处理计算得出研究区域内的NDVI。其次，采用欧洲航空局WorldCover v100土地覆盖数据（分辨率为10m），经Fragstats 4.2计算研究区域内的绿地组成指标。结果显示，研究区域内共识别出8种土地覆盖类型，即树木、灌木、草地、耕地、建筑用地、裸地／稀疏植被区、水体和草本湿地。考虑到灌木（0.001%）和草本湿地（0.013%）的面积占比较小，本文仅将树木、草地及耕地三个类型的面积占比纳入GSE指标。随后在Fragstats 4.2中计算树木、草地及耕地的整体景观格局指数作为配置维度指标。

2.2.2 目视视角下的城市GSE指标选取及数据获取

研究首先利用ArcGIS以200m的间隔沿一、二、三级道路选取79 777个观测点，使用百度街景地图捕捉观测点上0°、90°、180°和270°四个基本方向的图像（640 × 480像素），共计319 108张。随后，在Python 3.7中使用包含150个类别（如树木、建筑物、汽车等）的ADE20K数据库训练全卷积网络（FCN–8s）模型，对图像进行语义分割以获取其组成内容。用特定的颜色填充不同语义的像素，计算绿色植被所占的百分比，即绿视率（*GVI*）：

$$GVI = \frac{\sum_{i=1}^{m} Area_g}{\sum_{i=1}^{m} Area_t} \times 100\%, \quad (1)$$

式中，$Area_t$代表每张街景图中的总像素数量，$Area_g$表示该图中绿色植被所占像素的数量，m是在观测点获取的图像数量，在本研究中，m取值为4。

本文使用人机对抗评分评估公众对街景图像的感知质量。研究团队从街景图像数据库随机选择5 000张涵盖不同景观元素特征的街景图像构

表 1：鸟瞰视角下的 GSE 指标

分类	指标	描述
组成	植被归一化指数（NDVI）	· 反映地表植被密度和健康状况 · 数值越高，地表植被情况越好
	树木面积占比	网格中树木所占的面积比例
	草地面积占比	网格中草地所占的面积比例
	耕地面积占比	网格中耕地所占的面积比例
	景观面积占比（PLAND）	网格中全部绿地斑块所占的面积比例
配置	最大斑块指数（LPI）	· 网格中最大单一绿地斑块所占的面积比例 · 数值越接近 0，斑块越小
	斑块数量（NP）	· 网格中绿地斑块的数量 · 数值越高，斑块破碎程度越高
	边缘密度（ED）	· 网格中绿地斑块的总边缘长度和网格面积的比值 · 数值越高，斑块破碎程度越高
	形状指数（SHAPE）	· 所有绿地斑块形状指数（斑块周长除以同面积的圆周长）的平均值 · 数值越接近 1，形状越简单
	分维数（FRAC）	· 绿地斑块边缘复杂度的平均值 · 数值越接近 1，形状越简单
	斑块凝聚指数（COHESION）	· 绿地斑块聚集程度 · 数值越高越聚集

表 2：目视视角下的 GSE 指标

分类	指标	描述
绿量	绿视率（*GVI*）	人的视野中绿色植被覆盖所占的百分比
感知质量	种类丰富度	街道绿色空间内植物种类的多样性
	可步行性	街道环境对步行活动的支持程度
	可达性	人们能够轻松到达和使用街道绿色空间的程度
	设施便利性	街道绿色空间内提供的设施和服务的便利程度
	通透性	街道网络的连通性和开放性
	整洁度	绿色空间的清洁程度
	安全性	街道绿色空间的安全状况（包括犯罪率、夜间照明、紧急设施等客观因素，以及居民对街道氛围的主观感受）

建训练数据集（图2）。从景观、建筑和城市规划类高校研究人员，以及熟悉当地环境的沿街店铺人员中随机选取40名志愿者（男女比例1∶1）对7项街景图像感知质量指标进行线上打分，评分范围均为0（质量极低）~100（质量极高）。研究使用基于Python的随机森林模型对志愿者评分及不同街景元素的占比进行训练，并自动为街景图像数据集评分。每个网格的GSE指标数值为该网格内所有图像相应指标评分的均值。为了排除因样本中街景图像过少而导致的结果偏差，本研究剔除了观测点少于5个（即街景图像少于20张）的网格，最终得到有效样本共2 750个。

2.3 社会经济指标

研究表明，人口密度和人均地区生产总值（GDP）和房价水平与社会经济状况紧密关联[31]~[33]。房价水平作为反映社会经济水平的重要指标，在多项实证研究中展现了较好的信效度。例如，张金光使用房价作为家庭收入的指标，探讨了南京市中心城区GSE的可获得性、可达性和吸引力在空间和社会层面上的不平等性[34]。余思奇等人依托于房价指标揭示了南京市主城区不同社会经济群体在城市公园可达性方面的空间差异[35]。因此，本研究在空间分析中以房价水平为主要社会经济指标，以人口密度及人均GDP为协变量。研究团队通过2020年WorldPop数据库（分辨率为100m）获取人口密度数据；由南京市统计局2020年区级GDP及常住人口数量计算而得人均GDP；并通过在线房源和租赁平台链家网获取房价数据。首先，利用ArcGIS 10.3分割并计算每个网格内的人口密度均值。其次，以各网格所在行政区的人均GDP作为该网格的人均GDP。最后，计算每个网格内所有居住区的房价均值。

2.4 数据分析

在ArcGIS 10.3平台中，使用自然断裂法将鸟瞰–目视视角下的GSE指标数值分为7个等级并进行可视化，以评估研究区域内GSE的地理公平性。对于社会公平性，首先使用单变量局部莫兰指数（Moran's I）检验房价水平，结果为0.924（p=0.001），表明在研究区域内房价水平存在高度且正向的空间自相关性。随后分别对房价水平和GSE指标进行双变量局部莫兰指数检验及可视化空间关联分析。最后，使用最小二乘法（OLS）、空间滞后模型（SLM）、空间误差模型（SEM）及地理加权模型（GWR）四种模型对房价水平与GSE指标进行回归分析，并以人口密度和人均GDP为协变量。其中，OLS模型如公式（2）所示：

$$HP_i = \alpha_0 + \alpha_1 GS_i + \alpha_2 PO_i + \alpha_3 GDP_i + \varepsilon_0 \ , \qquad (2)$$

式中，HP_i、GS_i、PO_i和GDP_i分别表示第i个网格内的房价水平、GSE指标、人口密度和人均GDP；α_0和ε_0分别为常数项和误差项。

对每个GSE指标的OLS模型进行残差空间自相关检验，结果显示所有残差的莫兰指数均为显著正值（如以NDVI为自变量的OLS模型残差莫兰指数为0.878，p=0.001），表明现有的OLS模型未能有效充分捕捉数据中的空间结构特征。因此，本研究在公式（2）的基础上，基于距离权重构建空间回归模型SLM和SEM：

$$HP_i = \alpha_0 + \gamma W_i + \ \alpha_1 GS_i + \alpha_2 PO_i + \alpha_3 GDP_i + \varepsilon_0 \ , \qquad (3)$$

式中，附加项γW_i在SLM中表示邻近地区的空间滞后项，在SEM中表示邻近地区的误差项。在构建权重时，为确保每个网格至少有一个相邻网格，距离权重阈值使用了所需的最小距离，即864m。为了检验结果的稳健性，本研究使用1 000m的距离阈值并基于共点共边相邻和共边相邻构建权重以进行敏感性分析。

尽管SLM和SEM模型考虑了空间自相关问题，它们却只能解释研究区域内的全局空间关联。而GWR模型能在每一网格单元内为相关指标的回归系数提供局部估计，从而揭示空间异质性。因此，研究在Rstudio中使用spgwr包，运用交叉验证法计算得出最佳带宽约为485m，并基于此进行GWR模型分析。GWR模型如公式（4）所示：

$$\begin{aligned} HP_i = {} & \alpha_0(u_i, v_i) + \alpha_1(u_i, v_i) GS_i + \alpha_2(u_i, v_i) PO_i \\ & + \alpha_3(u_i, v_i) GDP_i + \varepsilon_0 \end{aligned} \ , \qquad (4)$$

式中，HP_i、GS_i、PO_i、GDP_i和ε_0的释义与公式（2）、公式（3）相同；

$\alpha_0(\mu_i, \nu_i)$是第i个网格的截距项，$\alpha_1(\mu_i, \nu_i)$、$\alpha_2(\mu_i, \nu_i)$和$\alpha_3(\mu_i, \nu_i)$是第i个网格的回归系数，它们的值均随地理位置(μ_i, ν_i)变化。

随后，本研究依据决定系数（R^2）和赤池信息量准则（AIC）等参数比较模型的拟合优度。GWR模型生成的系数估计图可以展示每个GSE指标的回归系数在研究区域内的变化，有助于识别对房价具有显著相关性的区域和GSE指标，并进一步揭示GSE在空间上的社会分异特征，对提出科学、精细化的暴露盲区“网格化”干预路径具有重要意义。

3 研究结果与讨论

3.1 GSE指标空间分布特征

在鸟瞰视角下，GSE组成指标均呈现了不均衡分布现象（图3）。其中，NDVI、树木面积占比及PLAND呈现出相似的空间模式，即中心建筑较密集区域的数值较低，靠近山体区域的数值较高；边缘区域数值普遍高于中心区域，表明边缘区域普遍绿化程度较高，GSE水平较高。草地面积占比和耕地面积占比的空间分布模式类似，中心区域数值普遍较低，包括靠近山体的区域；边缘区域数值相对较高。对于GSE配置指标，NP和LPI呈现相反的分布特征，整体而言中心区域的绿地小但数量多，东北部及边缘区域的绿地大而数量少。ED、SHAPE、FRAC和COHESION分布相对较均衡，绿地形状较为规则且聚集度较高。

在目视视角下，绿量及感知质量存在分布失衡现象（图4）。GVI、种类丰富度和通透性指标与NDVI具有相似的空间模式，即边缘区域的数值普遍高于中心建筑密集区，说明边缘区域绿化相对较好且街道较为开敞；可步行性、可达性、设施便利性、整洁度和安全性指标具有类似的空间分布模式，指标数值普遍较高，表明研究区域内街景感知质量普遍较高。

3.2 GSE指标与房价的空间关联

研究区域内古都文化核及河西片区的房价水平最高，向外围呈逐渐递减趋势（图5）。双变量局部莫兰指数检验结果显示（图6），莫兰指数的绝对值越大，则暴露指标与房价在空间上具有更强的空间相关性。结果显示，19个GSE指标均与房价呈现显著的空间相关性，其中仅草地面积占比、耕地面积占比、NP及种类丰富度与房价呈现负空间相关性。这一结果表明，绿地条件越好（以树木为主，数量多且质量好）、绿地越大、形状越多样化且凝聚度越高，房价水平则越高。此外，从系数来看，房价水平与鸟瞰视角下GSE指标的莫兰指数绝对值普遍低于其与目视视角下GSE指标的莫兰指数绝对值。其中，鸟瞰视角下树木面积占比与耕地面积占比的莫兰指数绝对值较高，分别为0.129和0.171，而目视视角下莫兰指数绝对值较高的设施便利性、整洁度和可达性分别为0.292、0.254和0.232。此研究结果表明，房价水平与GSE绿量及质量密切相关，与现有多项探索城市公园绿地特征与房价水平关联的研究结果一致[36][37]。

表3展示了鸟瞰–目视视角下不同GSE指标的四种回归模型分析结果。整体而言，空间回归模型（SLM、SEM和GWR）的拟合程度远优于OLS，其中SLM和SEM拟合优度最好，GWR模型次之。在使用不同权重方式的敏感性分析中，SLM和SEM模型的回归结果与表3所报告的结果高度一致，R^2均高于0.9。这一结果验证了研究结果的稳健性，再次证明了GSE与房价水平存在显著的空间效应。

3.3 GSE指标与房价的空间关联及分异特征

结果显示（图7，8），研究区域内所有GSE指标的系数估计均有正有负，且负值所占面积可观，表明GSE存在显著的社会公平性分异。结合房价分布特征（图5），高房价区域在鸟瞰视角下的NDVI、树木面积占比、PLAND、LPI、ED、SHAPE的系数估计值为正值，说明在该区域中，随着植被覆盖面积的增加、绿地规模的增大、绿地形状的多样化及与周边环境联系的紧密性增强，房价逐渐增高。同时，高房价区域在目视视角下的街道空间的GVI、可步行性、可达性、设施便利性、整洁度、安全性的系数估计为正值，表明该区域中随着街道空间绿量及街景感知质量的提升，房价水平逐步提升。反之，低房价区域中这些指标的系数估计为负值，意味着这些区域中GSE与房价呈负相关。这一结果可能由这些区域的地理位置所决定：低房价区域普遍位于中心城区的边缘区域，绿地条件较好，因此较之于GSE的增加，城市化水平的提升或许更能够拉高房价水平。街道绿量与街道品质也曾在现有研究中被证实与房价相关联。白钊成等人通过研究杭州市中心城区街道绿量的社会分异，揭示了街道绿量与房价呈现正相关[38]。李莹等人在一项以广州市为例的研究中发现，街道品质特征对房价的影响可达36.74%[39]。此外，本研究中大部分高房价区域内的草地面积占比、耕地面积占比、NP、种类丰富度、通透性的系数估计为负值，说明在高房价区域中建筑密度低、城市化水平低的片区，房价水平相对较低。

3.4 GSE规划干预策略

通过上文的分析，本研究发现目视视角下的GSE指标与社会经济水平的空间相关程度普遍高于鸟瞰视角。因此，在制定以促进“绿色公平”为导向的规划举措时，应优先考虑提升街道空间的绿量及质量。在微观层面，结合GSE指标的地理公平性及社会公平性空间分异特征，本研究识别了亟待优化的低GSE区域，并为此区域内的高社会经济水平片区和低社会经济水平片区①分别提供优化策略。

① 通过图 4 研究区域内房价水平的空间分布界定高 / 低社会经济水平片区，黄色为中等水平，蓝色越深，表明社会经济水平越低，红色越深，则社会经济水平越高。

表 3：鸟瞰 – 目视视角下 GSE 指标与房价水平的拟合结果

自变量	OLS			SLM			SEM			GWR	
	R^2	*AIC*	对数似然	R^2	*AIC*	对数似然	R^2	*AIC*	对数似然	R^2	*AIC*
鸟瞰视角											
NDVI	0.131	− 3 948.410	1 978.210	0.939	− 10 480.800	5 245.420	0.939	−10 477.500	5 242.766	0.903	− 9 688.662
树木面积占比	0.136	− 3 964.150	1 986.070	0.939	− 10 481.700	5 245.830	0.939	−10 477.000	5 242.495	0.903	− 9 696.385
草地面积占比	0.107	− 3 872.520	1 940.260	0.938	− 10 457.700	5 233.830	0.938	−10 459.700	5 233.833	0.905	− 9 735.061
耕地面积占比	0.111	− 3 885.630	1 946.820	0.938	− 10 458.200	5 234.100	0.939	−10 461.800	5 234.890	0.904	− 9 705.012
PLAND	0.135	− 3 960.390	1 984.200	0.939	− 10 492.000	5 251.000	0.939	−10 485.200	5 246.622	0.904	− 9 699.222
NP	0.139	− 3 973.290	1 990.840	0.940	− 10 524.300	5 267.600	0.939	−10 506.100	5 257.050	0.905	− 9 742.258
LPI	0.136	− 3 965.890	1 986.950	0.939	− 10 498.000	5 254.010	0.939	− 10490.000	5 248.996	0.905	− 9 716.672
ED	0.108	− 3 876.800	1 942.400	0.938	− 10 459.800	5 234.920	0.939	−10 462.700	5 235.339	0.901	− 9 641.370
SHAPE	0.129	− 3 942.570	1 975.280	0.939	− 10 495.000	5 252.510	0.939	−10 476.300	5 242.135	0.903	− 9 960.407
FRAC	0.111	− 3 886.590	1 947.290	0.939	− 10 465.600	5 237.820	0.939	−10 462.200	5 235.102	0.898	− 9 528.610
COHESION	0.130	− 3 946.140	1 977.070	0.939	− 10 512.700	5 261.350	0.939	−10 501.800	5 254.885	0.604	− 6 100.009
目视视角											
GVI	0.125	− 3 930.530	1 969.260	0.939	− 10 471.400	5 240.720	0.939	−10 469.900	5 238.950	0.902	− 9 655.261
种类丰富度	0.107	− 3 873.060	1 940.530	0.939	− 10 465.800	5 237.910	0.939	−10 474.500	5 241.269	0.862	− 8 877.027
可步行性	0.126	− 3 931.390	1 969.690	0.938	− 10 458.300	5 234.140	0.938	−10 459.400	5 233.694	0.895	− 9 514.691
可达性	0.153	− 4 016.13	2 012.060	0.938	− 10 457.100	5 233.540	0.938	−10 454.600	5 231.292	0.881	− 9 235.790
设施便利性	0.173	− 4 083.690	2 045.850	0.938	− 10 460.200	5 235.110	0.938	−10 454.800	5 231.394	0.889	− 9 090.944
通透性	0.109	− 3 836.550	1 922.280	0.938	− 10 354.400	5 182.220	0.938	−10 357.200	5 182.623	0.864	− 8 838.506
整洁度	0.162	− 4 049.470	2 028.740	0.938	− 10 464.700	5 237.370	0.938	−10 459.700	5 233.835	0.846	− 8 614.218
安全性	0.152	− 3 971.400	1 989.700	0.938	− 10 359.600	5 184.820	0.938	−10 357.300	5 182.643	0.872	− 9 062.314

注

表中所有 GSE 指标的 GWR 模型的 R^2 为全局平均值，且不存在对数似然项。

1）低GSE－高社会经济水平区域。此区域内GSE与社会经济水平呈负向关联，典型特征是自身房价高，但绿地数量少，规模较小且形状规则，整体植被覆盖情况不佳。此特征多出现在发展较好、生活水平较高的城市区域。此类区域可利用的土地资源稀缺，导致绿地“增量”难度极大，因此可考虑通过调整绿地结构，如改善绿地形状，提升居民接触绿地的机会。绿地斑块形状越复杂，绿地边界与周边环境耦合度越高，居民接触到绿地的机会越多。此外，可结合道路、河流等线型空间打造绿色廊道，增加破碎绿地的连接度，提升城区整体GSE水平。

2）低GSE－低社会经济水平区域。此区域内GSE与社会经济水平呈正向关联，普遍处于研究区域边缘区域且本身房价不高，城市活力相对较低；同时，此类区域内的草地、耕地占比高于树木。由上文可知，草地、耕地面积占比和社会经济水平呈现负空间相关性，而树木面积占比与社会经济水平呈现正空间相关性。因此，此类区域内“增绿”的发展重点应放在增植树木，可考虑在草地上适当增加乔灌木，增加视觉上景观层次的同时，提升GSE质量。

4 研究结论与展望

本研究从鸟瞰－目视视角构建了城市GSE综合评估模型，以房价表征居民社会经济水平，使用OLS、SLM和SEM模型对南京市中心城区的GSE进行了地理和社会公平性测度。为了更细致地测度GSE社会公平性的空间分异，本研究基于GWR模型对GSE与房价的空间关联进行网格单元可视化。

结果表明，研究区域内的GSE在空间分布上存在不均衡现象，中心区域绿地碎片化程度高，整体GSE程度低于边缘区域。房价与GSE指标存在显著的空间关联，目视视角下的GSE指标与房价水平的空间相关程度普遍高于鸟瞰视角。其中，草地面积占比、耕地面积占比、NP及种类丰富度与房价呈现负相关，其余GSE指标与房价呈现正相关。此外，SLM和SEM模型在GSE指标预测房价水平的模型中拟合效果最好。GWR模型结果进一步表明，南京市中心城区的GSE无论在地理公平性层面亦或是社会公平性层面均存在显著的失衡现象。

本研究精准定位了城市GSE不足的区域，针对性地对低GSE－高社会经济水平区域及低GSE－低社会经济水平区域分别提出了科学规划干预举措。本研究进一步扩展了暴露生态学理论的实证研究，在实践上有助于推进城市GSE评估，对通过城市规划和绿地系统规划以促进GSE的公平性具有指导性价值。

本研究存在以下不足。首先，评估目视视角中的感知质量指标时，对街景图像训练集进行打分的志愿者的数量、职业构成、年龄分布等差异可能对结果造成一定的误差，未来研究需对这些因素进行控制以提升结果的稳健性。其次，选取社区房价来表征社会经济水平具有一定的局限性，未来可结合社区平均收入和教育程度等指标全面衡量社会经济水平。再者，基于横截面数据的分析结果无法揭示“GSE－房价水平”之间的因果效应，未来研究可采用长时间序列的数据弥补此不足。最后，高密度城市区域的样本选取限制了规划调控举措的普适性，未来研究需进一步扩大研究区域，考虑多尺度、多时空、跨区域背景下的GSE公平性分异。

图 1. 研究区域区位图
图 2. 街景图像及其语义分割结果示例
图 3. 鸟瞰视角下 GSE 指标的空间分布
图 4. 目视视角下 GSE 指标的空间分布
图 5. 研究区域内房价水平的空间分布
图 6. 房价水平与不同 GSE 指标的空间相关性
图 7. 基于 GWR 模型的房价水平与鸟瞰视角下 GSE 指标的系数估计
图 8. 基于 GWR 模型的房价水平与目视视角下 GSE 指标的系数估计